Volume 8, No. 5, May – June 2017
International Journal of Advanced Research in Computer Science
RESEARCH PAPER
Available Online at www.ijarcs.info
ISSN No. 0976-5697

Efficient Image Haze Removal using Aging Particle Swarm Optimization based Dark Channel Prior

Jaswinder Kaur
Department of Computer Engineering and Technology
Guru Nanak Dev University
Amritsar, India

Prabhpreet Kaur
Department of Computer Engineering and Technology
Guru Nanak Dev University
Amritsar, India

Abstract: Haze reduces the visibility of a scene. Haze removal is one of the challenging tasks as it depends upon the unknown depth information. This paper presents an efficient method to remove haze from a single image based on the aging particle swarm optimization and dark channel prior. In the proposed method firstly, thickness of the haze is evaluated using dark channel prior, then aging particle swarm optimization is used to monitor and locate the best optimized value for restoration. The adaptive histogram equalization is applied to increase the contrast of the degraded image. An enhanced and optimized image is obtained. Some standard parameters such as mean square error, peak signal to noise ratio and bit error rate are utilized to compare the existing and proposed method. This method is useful for many computer vision and image understanding applications. The experimental results demonstrate that the proposed approach provides higher quality results.

Keywords: haze, dark channel prior, aging particle swarm optimization, airlight, adaptive histogram equalization.

I. INTRODUCTION

The quality of outdoor images is usually degraded [1], because the light getting absorbed or dispersed from the atmospheric particles in the existence of fog, haze or smoke. The degraded images lose contrast and color fidelity [2]. Hence, the visibility of the scene is reduced. Many automatic systems have failed to work, which highly depend to the input images. Therefore, enhancing the entire process of image dehazing will benefit several computer vision and image understanding applications [3] like image classification [4-6], aerial imagery [7], video/image retrieval [8-10], object detection and remote sensing [11]-[12], video analysis and recognition [13-15]. However, haze eliminating is one of the difficult tasks as it depends upon the unknown depth information [16].

Earlier analysts used the traditional methods to eliminate the haze from a single image, i.e. dehazing techniques based on histogram [17]-[18]. Since, a single image could not provide more information. Eventually, analysts made an effort to enhance the dehazing results using multiple images. Schechner et al. [19]-[20], proposed polarization based methods, where several images were taken with various levels of polarization. Narasimhan et al. [21]-[22] proposed dehaze method with many images under the similar atmospheric conditions.

Later, major improvement had been made by using the physical model. Tan [23] introduced an automatic method that just needed a single input image. The image contrast was maximized according to Markov Random Field (MRF). Even though Tan's method obtained better results. However, the disadvantage was that it tends to generate oversaturated pictures. Fattal [24] proposed Independent Component Analysis (ICA) to remove haze from the color images. But, this method took more time as well as not applicable for grayscale images. Chavez [25] motivated from the dark object subtraction method, He et al. [26] proposed an easy method, and a successful picture of the Dark Channel Prior (DCP) to eliminate the haze out of the picture and restored dehaze image using an atmospheric scattering model. This method needed the soft mating to refine transmission map, which took more time. However, it also could not effectively handle the sky images. To overpower the weak spot of the Dark channel prior (DCP) method, improved [27]-[28] algorithms were proposed Tarel et al. [27] introduced a fast visibility restoration of the single input image. This method had high speed and ability to handle both gray and color images. Liu et al. [28] presented a better dark channel prior for sky and non-sky areas, and more natural images were restored. For effectiveness, Gibson et al. [29] Yu et al. [30], Tarel and Hautiere [27], He et al. [31], replaced the soft matting of Levin et al. [32] which took more time with a standard median filter, median of a median filter, guided image filter respectively. Bo et al. [33] proposed fast single image dehazing using a bilateral filter. In terms of dehazing quality, Nishino et al. [34] presented the new Bayesian probabilistic method usually estimated the modern scene albedo as well as level through just one hazy picture by completely leveraging their latent mathematical structure, but it tends to over enhance the contrast on some occasions. Guo et al. [35] proposed the parameter selection approach, for single image defogging based on Genetic Algorithm. But according to qualitative and quantitative analysis Guo et al. results were not much efficient. Regardless of the impressive progress, there are several issues with the existing techniques.

Figure 1. An overview of proposed dehazing approach. Top-left: original hazy image. Top-right: dark channel prior. Bottom-left: Transmission filtered map. Bottom-right: picture without haze.

This paper presents the following. Part 2, presents an overview of the dark channel prior which is related to our propose work. Part 3, explains the proposed haze removal techniques. Part 4, represents the Methodology flowchart. Part 5, presents the qualitative and quantitative experimental results. Finally, part 6, presents the conclusion and future work.

II. BACKGROUND

The dark channel prior and optical model of hazy images is closely related to our proposed work [1], [26], [36].

A. *Optical model of hazy image*

The below formula defines the occurrence of the hazy images:

$$I(u) = j(u)t(u) + A(1 - t(u)) \tag{1}$$

where I is the original hazy picture, u is the pixel index, j is an image without haze, the transmission map is t, indicates the portion of light which is not dispersed, and A is generally the atmospheric light. The initial expression $j(u)t(u)$ is known as direct attention and the second expression is known as $A(1-t(u))$ airtight.

B. *Dark channel prior*

The dark channel prior approach depends on the observation, in which a few pixels possess very low intensity within a minimum of one color channel. The main process of image dehazing is to approximate the transmission map t and atmospheric light A from hazy picture. To estimate both the atmospheric light A and transmission t, He K. et al. initially proposed the dark channel prior method. The dark channel $j^{dchannel}$ for a random image j is shown as:

$$j^{dchannel}(u) = \min_{v\varepsilon\Omega(u)}\left(\min_{c\varepsilon(r2,g2,b2)} j^c(v)\right) \tag{2}$$

where j^c defines the r2 (red), g2 (green), b2 (blue) color channel of the original picture j and $\Omega(u)$ is the regional patch origin at u. Two minimum operators are: $\min_{c\varepsilon(r2,b2,g2)}$ is the minimum operator to examine the minimum value in the three color channels and $\min_{v\varepsilon\Omega(u)}$ is the minimum filter.

C. *Transmission Estimation*

If j is a dehazed picture, excluding sky regions, then the dark channel associated with j is commonly approached to zero:

$$j^{dchannel} \to 0 \tag{3}$$

Haze image equation (1) is normalized by A to estimate the atmospheric light.

$$\frac{I^c(u)}{A^c} = t(u)\frac{j^c(u)}{A^c} + 1 - t(u) \tag{4}$$

we suppose that the transmission map within a regional patch $\Omega(u)$ is actually constant. Then, this transmission is represented as $t2(u)$. Hence, the dark channel can be computed from both sides of the equation (4). Put two minimum operators on both sides:

$$\min_{v\varepsilon\Omega(u)}\left(\min_{c}\frac{I^c(v)}{A^c}\right) = t2(u)\min_{v\varepsilon\Omega(u)}\left(\min_{c}\frac{j^c(v)}{A^c}\right) + 1 - t2(u) \tag{5}$$

The dehaze image is j, whose dark channel is always tending to zero, due to dark channel prior:

$$j^{dchannel}(u) = \min_{v\varepsilon\Omega(u)}\left(\min_{c} j^c(v)\right) = 0 \tag{6}$$

Since A^c is being often positive, and tends to:

$$\min_{v\varepsilon\Omega(u)}\left(\min_{c}\frac{j^c(v)}{A^c}\right) = 0 \tag{7}$$

Putting (7) into (5), multiplicative terms can be removed and transmission $t2$ can be approximated as shown:

$$t2(u) = 1 - z\min_{v\varepsilon\Omega(u)}\left(\min_{c}\frac{I^c(v)}{A^c}\right) \tag{8}$$

where z is a constant value in order to maintain a tiny amount of haze (0<z<1). The transmission map is directly provided by this equation.

D. *Restoration of Input Image*

Finally, the picture is restored using below equation:

$$j(u) = \frac{I(u)}{\max(t(u), t_0)} + A \tag{9}$$

t_0 denotes the threshold of transmission $t(u)$ and is taken as 0.1.

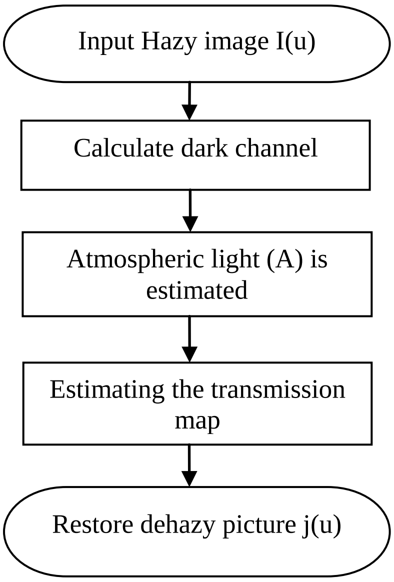

Figure 2. Flow diagram of dark channel prior [1]

III. PROPOSED TECHNIQUES

The proposed method is Aging Particle Swarm optimization using dark channel prior and adaptive histogram equalization is applied to enhance the picture contrast. The flow diagram of the proposed method is shown in Fig. 5. The detail of each process is explained in the below sub-sections.

A. *Adaptive histogram equalization*

The Adaptive histogram equalization (AHE) process is an advancement in the existing histogram equalization technique. The AHE has been often used to get better contrast images. It improves the inequality associated with pictures through modifying the values within the intensity image. In comparison to histogram equalization, it is implemented on very small data regions (tiles) instead of the whole image [37], [38].

B. *Proposed algorithm*

The Aging particle swarm optimization is a population dependent search method, influenced by the social interaction of the bird flocks. The age (Θ) and the lifespan (Φ) of the gbest particle are adaptively altered with respect to its leading power. Whenever the lifespan of the gbest is exhausted, then it is exchanged by newly developed particles. [39], [40], [41].

The operation of Aging Particle Swarm Optimization is shown as:

- Initialization: Initialize all the particles developed in the search space, velocities initialized to 0. The best particle in the search space is selected as the gbest. The lifespan and the age of the gbest particle is set in order $\Phi=\Phi_0$ and $\Theta=0$ respectively.

- Updating Velocity: Every particle velocity is updated according to the given equation:

$$v_j = w_{j-1} + c_{11} * r_{11} * \left(pbest_j - p_j\right) + c_{22} * r_{22} * \left(gbest_j - p_j\right) \quad (10)$$

  where v_j and p_j are current velocity and position of particles and v_{j-1} is previous velocity of the j^{th} particle. The $pbest_j$ and $gbest_j$ are the position of a j particle having best value found so far, within the entire population; the convergence behavior of the aging PSO is controlled by w; r_{11} and r_{22} are arbitrary parameters vary from [0, 1]; c_{11} and c_{22} manage how long a particle proceeds in a single iteration.

- Position Updating**:** The position of the entire particles updated with the successive iteration in the unit time interval is as:

$$p_j = p_{j-1} + v_j \quad (11)$$

- Updating pbest and gbest**:** When the position of the newly generated particle p_j is better than the $pbest_j$, then it becomes the new $pbest_j$. If in this iteration the best position is generated, then the $gbest_j$ can be updated to the newly best position. Here the $gbest_j$ represents the best solution.

$$pbest_j = p_j \ if \ \left(p_j\right) > \left(pbest_j\right)$$
$$gbest_j = g_j \ if \ \left(g_j\right) > \left(gbest_j\right)$$

- Lifespan control: Immediately after updating the position of all particles, the leading power of the gbest increase the performance of the entire swarm. The lifespan (Φ) is modified through a lifespan controller and the age (Θ) is increased by 1. When Θ> Φ i.e. lifespan is exhausted, then move to step 6. Otherwise, move to step 8.

- Creating a challenger: To challenge the gbest, a new particle is created by the challenger.

- Evaluate the challenger: If a newly created challenger possesses more leading power, then it becomes the new gbest by replacing the old gbest. The lifespan and the age of the new gbest are initialized to $\Phi= \Phi_0$ and $\Theta=0$ respectively.

- Termination Checking: When the number of iterations (FE) is greater than the maximum predefined iteration (maxi-evaluation), then the algorithm terminates. Otherwise the new iteration starts from step 2.

The proposed aging particle swarm optimization algorithm mainly performs three tasks.

- Firstly the lifespan of the gbest is adjusted by the lifespan controller based on its leading power.
- Secondly, a new particle is created to challenge the old gbest particle.
- Finally a qualifying criterion is used to determine whether the created particle is accepted as a new gbest
- Lifespan controller: The main function of lifespan controller is to control the leading power of the gbest. If the gbest has best leading power, then the controller increases its lifespan, otherwise, reduces its lifespan.

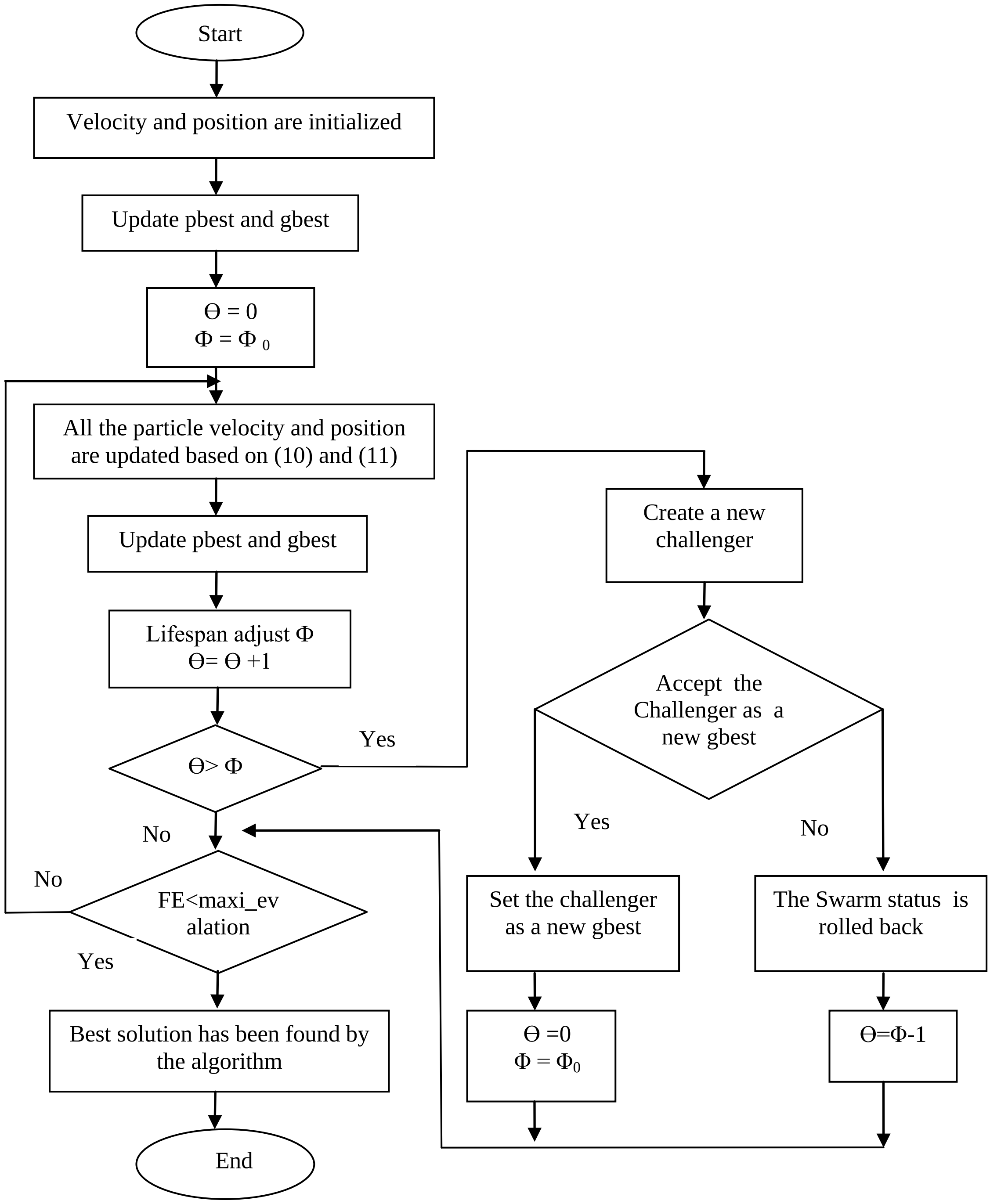

Figure 3. Flow diagram of proposed aging particle swarm optimization algorithm [40]

IV. PROPOSED METHODOLOGY

Fig. 5 shows the methodology of the proposed method. The haze is not removed by existing methods efficiently. Therefore, we propose the new techniques which consist of the dark channel prior, adaptive histogram equalization and aging PSO. The working of the proposed method is defined as:

- Firstly, hazy image is passed to the system shown in fig. 4.

Figure 4. Original hazy image.

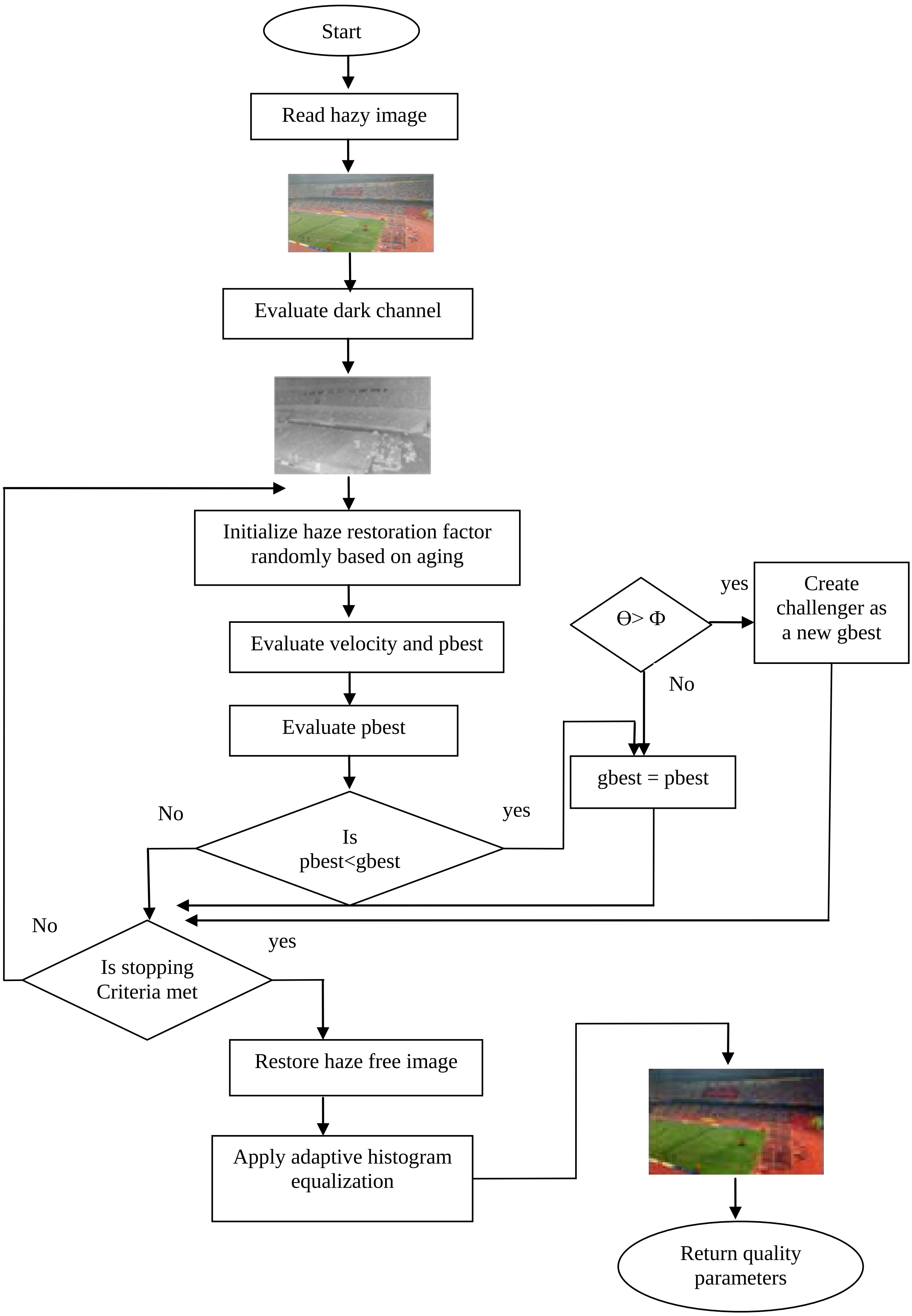

Figure 5. Flow diagram of proposed haze removal methodology.

- The thickness of haze is computed by applying dark channel prior to the hazy image.

Figure 6. Dark channel prior of hazy image

- Initialize the haze restoration factor randomly based on aging.
- The position and velocity of every particle are evaluated and compare with the best particle.
- If the position of the newly generated particle is better than, $pbest_j$ then it becomes new $gbest_j$.
- The dehaze image is restored using restored equation (9).
- Finally, the adaptive histogram equalization is applied to increase the contrast of the images.

Figure 7. Haze free image.

- The quality parameters are returned.
- If the lifespan of the gbest particle is exhausted, then the challenger creates a new particle, which is being accepted as a new gbest, and step from 6 to 8 are repeated.
- If the number of iterations is low, than the chosen, then steps from 4 to 8 are repeated.

V. EXPERIMENTAL RESULTS

The proposed algorithm is designed and executed in the MATLAB R2013a environment utilizing an image processing toolbox on a i5-2.50GHz PC with 8 GB RAM. To show the effectiveness of the proposed method, it has been tested on many benchmark images as well as qualitatively compare with He et al.'s [26], Nishino et al. [34], and Guo et al. [35] method

The dataset is collected from: http://www.cs.huji.ac.il/~raananf/projects/dehaze_cl/results/. http://perso.lcpc.fr/tarel.jean-philippe/.
Many (3000) road hazy images are collected from FRIDA dataset.

A. Qualitative comparison of hazy images

Good results are given by all the dehazing algorithms, but it is very complicated to rate them visually. In order to compare them various benchmark images are taken, which consist of large gray and white region, because some existing methods are unable to detect white regions.

Fig. 8 indicates the qualitative evaluation along with the existing three state-of-the-art dehazing methods [26], [34], [35] on benchmark hazy images. Fig. 8 (a) shows original hazy pictures Fig. 8 (b-d) depicts final results of He et al. [26], Nishino et al. [34], and Guo et al. [35], respectively. The proposed algorithm results are given in Fig. 8 (e). Almost all the haze is eliminated from Nishano's final results, and also objects are well restored. But it suffers from over enhancement. It has been shown in Fig. 8 (c) the restored pictures are suffering from distortion and over saturation; particularly in the fifth picture of the swan (shade of the swan is usually modified to dark). On the other hand, the final results of He et al. is looking good (shows Fig. 8 (b)). There are no halo artifacts and the thick haze within the distance is well eliminated. But in the white object regions color distortion still appeared. This algorithm cannot handle the sky regions (shown in Fig. 8 (b) sixth image of the mountain) and also tends to overestimate the particular transmission.

Results of Guo et al. Fig. 8 (d) are visually good but cannot effectively remove the haze. Guo tries to improve the performance of He et al. and Tarel et al. [27] by selecting the different parameters. In comparison to the three existing algorithms, proposed algorithm final results are totally free of oversaturation. As shown in Fig. 8 (e), the cloud as well as the sky in the pictures is evident and the mountains are improved moderately.

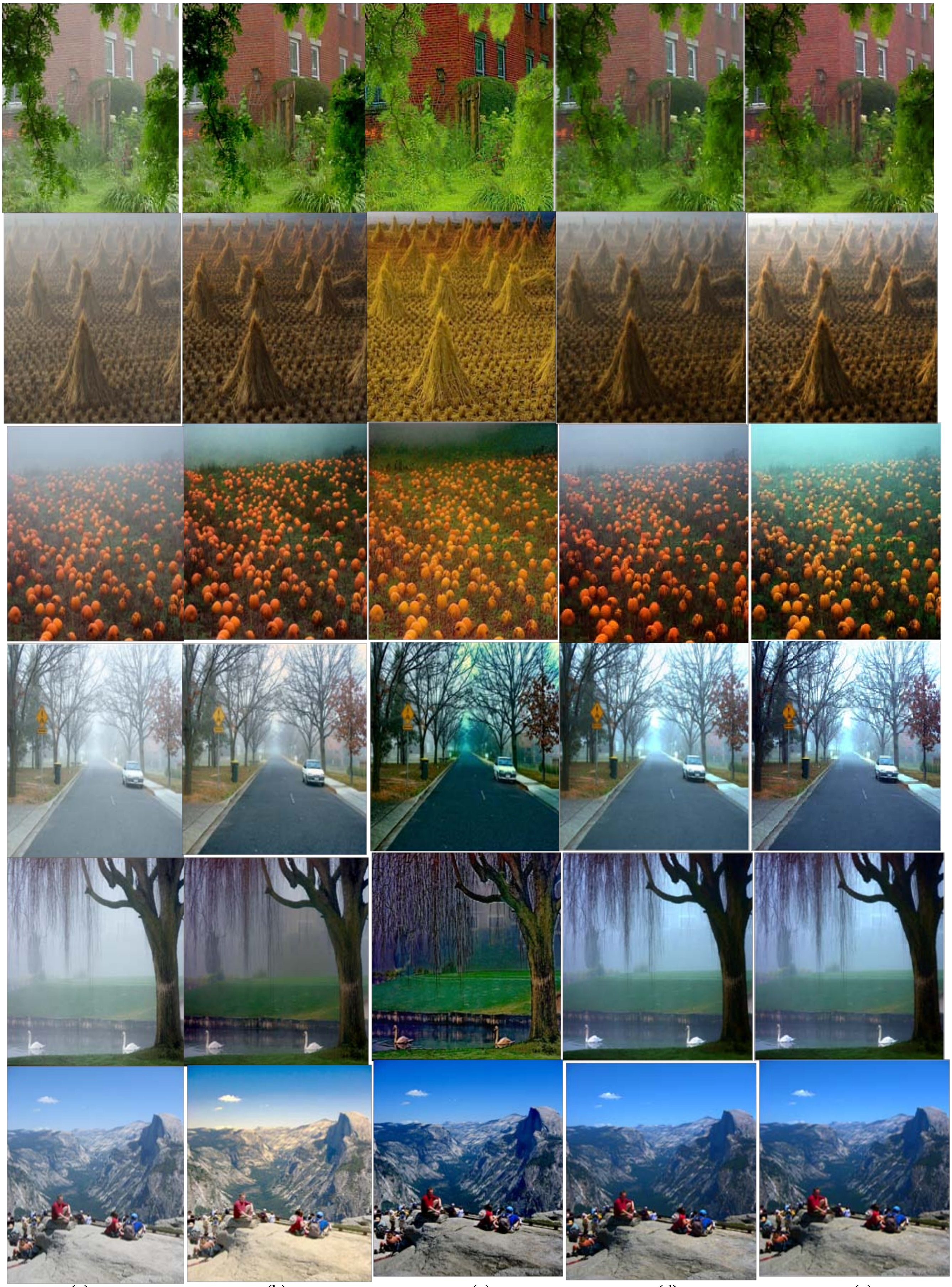

(a) (b) (c) (d) (e)

Figure 8. Shows qualitative comparison of various techniques on benchmark hazy images (a) The hazy images. (b) He et al.'s results [26] (c) Nishino et al.'s results [34]. (d) Guo et al.'s results [35]. (e) Proposed result

B. *Quantitative comparison of hazy images*

Fig. 9 shows a quantitative comparison of the existing Guo et al. [35] and proposed algorithm. Fig. 9 (a) presents the hazy picture. Fig. 9 (b) shows the Guo et al. results [35] and Fig. 9 (c) indicates the final results of the proposed algorithm. To further prove the overall performance of the aging particle swarm optimization and its advantage over the existing approach, the quantitative evaluation is also conducted on hazy images depicts in Fig. 9.

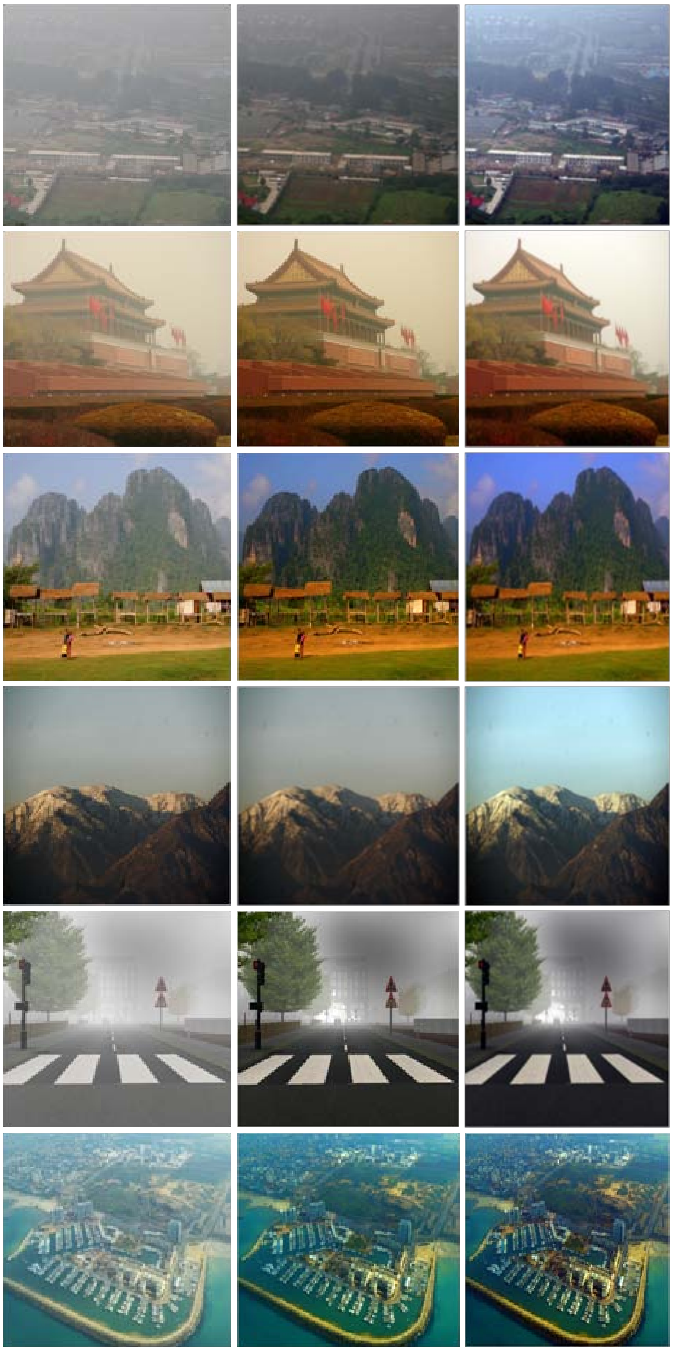

(a) (b) (c)

Figure 9. Shows quantitative comparison of various images. (a) hazy picture to be dehazed (b) Guo et al [35] approach (c) proposed approachThe proposed method is examined based on some parameters, i.e. Peak Signal to Noise Ratio (PSNR), Mean Square Error (MSE) and Bit Error Rate (BER). The final results demonstrate that the proposed approach is superior to existing one.

- Mean Square Error: For better result mean square error must be reduced. The mean square error provides the cumulative error for the original hazy image and output image. The less MSE, results in a minimum error. The mean square error is measured as [42]:

$$MSE = \Sigma m,n\left(M_{in}\left(m,n\right) - N_{op}\left(m,n\right)\right)^2 \qquad (12)$$

where, m and n are the number of rows and columns of the input picture respectively. M_{in} is the input image and N_{op} is the output image.

- Peak signal to noise ratio: The peak signal to noise ratio provides the quality measurement of the original input image and restored enhance image. The greater value of PSNR shows a better quality image. The PSNR can be computed using the below equation. [42]:

$$PSNR = 10\log_{10}\left(\frac{R}{MSE}\right) \qquad (13)$$

where R is maximum fluctuation in the original input image.

- Bit error rate: The bit error rate must be minimized for better result. The less value of BER shows a better quality image. It is defined as [42]:

$$BER = \frac{Number\ of\ errors}{Number\ of\ bits\ send} \qquad (14)$$

It can be measured as:

$$BER = \frac{1}{PSNR} \qquad (15)$$

Table I. Evaluation of Mean Square Error

Image name	*Image resolution*	*Existing method [35]*	*Proposed method*
canon	600×525	0.6093	0.0186
hut	600×450	0.1858	**0.0063**
mount	512×384	0.1434	**0.0161**
snow	876×584	0.0936	**0.0507**
road	640 ×480	0.2642	**0.0506**
sea	1600×928	0.4070	**0.0429**

Table II. Evaluation of Peak signal to noise ratio

Image name	*Image resolution*	*Existing method [35]*	*Proposed method*
canon	600×525	50.2821	**65.4433**
Hut	600×450	55.4403	**70.1090**
mount	512×384	56.5656	**66.0551**
Snow	876×584	58.4180	**61.0821**
Road	640 ×480	53.9115	**61.0923**
sea	1600×928	52.0349	**61.8101**

Table III. Evaluation of Bit Error Rate

Image name	***Image resolution***	***Existing method [35]***	***Proposed method***
canon	600×525	0.0199	**0.0153**
Hut	600×450	0.0180	**0.0143**
mount	512×384	0.0177	**0.0151**
snow	876×584	0.0171	**0.0164**
road	640 ×480	0.0185	**0.0164**
sea	1600×928	0.0192	**0.0162**

Table 1, Table 2 and Table 3 compares the MSE, PSNR and BER of Existing [35] and proposed method. The proposed method shows better quantitative results.

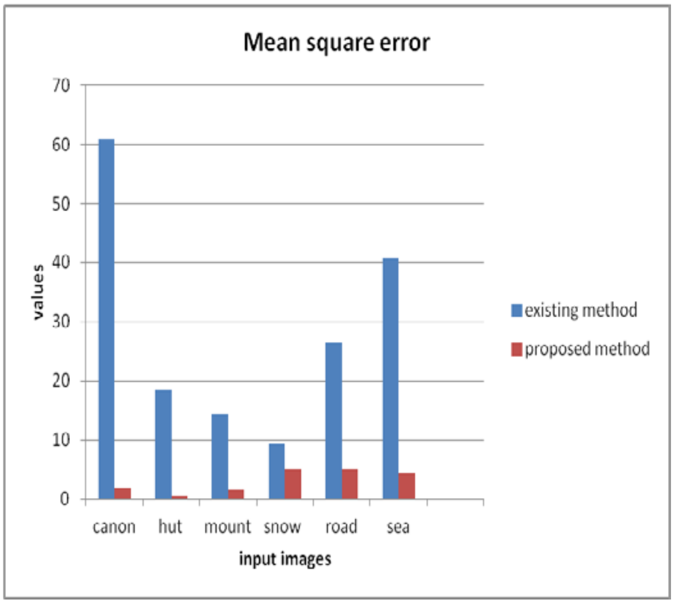

Figure 10. Mean Square error of existing and proposed method.

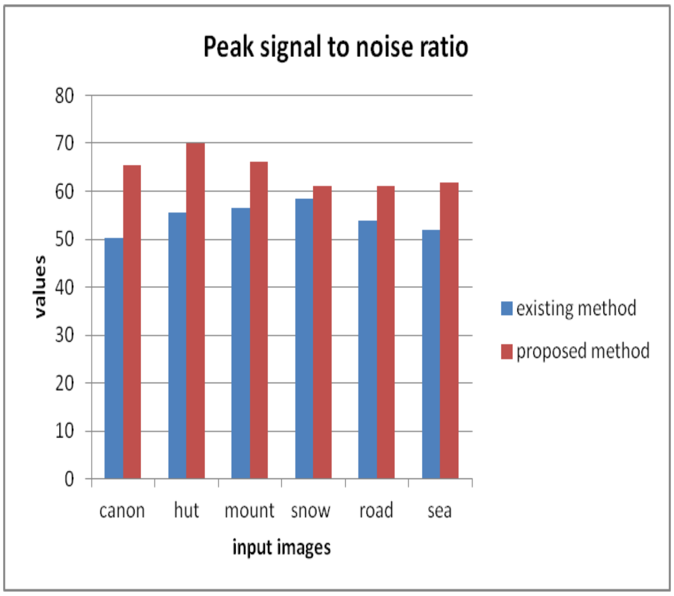

Figure 11. Peak signal to noise ratio of existing and proposed method.

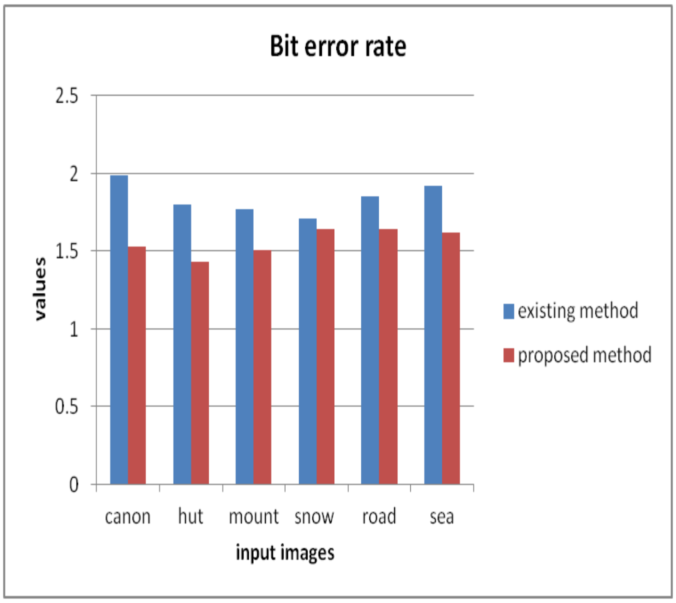

Figure 12. Bit error rate of existing and proposed method.

Fig. 10, Fig. 11 and Fig. 12 indicates a comparative evaluation with the MSE (mean square error) PSNR and BER associated with an existing approach (blue color) and Proposed Approach (red color) of various images. The Graph shows decrease in MSE, BER and increase in PSNR value for every image utilizing the proposed method. This presents a vast improvement within image quality.

VI. CONCLUSION

A new, single image dehazing technique is presented that maximize the visibility of the hazy image. The proposed methodology integrates dark channel prior and aging particle swarm optimization. The proposed algorithm tries to find the best solution in the entire search space. The contrast of the hazy images is enhanced using Adaptive histogram equalization. The Aging PSO removes the limitations of the existing methods. The proposed method is tested on various benchmark hazy images. The experimental results demonstrate that the proposed approach provides higher quality dehaze images. The quantitative measurements like PSNR, MSE and also BER verifying the efficiency of the proposed method over the existing Genetic algorithm. The new method is applicable in many computer vision and image understanding applications. We would like to extend our work to remote sensing hazy images.

VII. REFERENCES

[1] Y. Xu, X. Guo, H. Wang, F. Zhao, L. Peng, "Single Image Haze Removal Using Light and Dark Channel Prior," Communications in China (ICCC), 2016 IEEE/CIC International Conference on, 2016. doi: 10.1109/ICCChina.2016.7636813

[2] Q. Zhu, S. Yang, P. A. Heng, X. Li, "An Adaptive and Effective Single Image Dehazing Algorithm Based on Dark Channel Prior," Robotics and Biomimetics (ROBIO), 2013 IEEE International Conference on, 2013, pp. 1796-1800. doi: 10.1109/ROBIO.2013.6739728

[3] Q. Zhu, J. Mai, L. Shao, "A Fast Single Image Haze Removal Algorithm Using Color Attenuation Prior," IEEE Transactions on Image Processing, vol. 24, no. 11, pp. 3522-3533, November 2015. doi: 10.1109/TIP.2015.2446191

[4] L. Shao, L. Liu, X. Li, "Feature Learning for Image Classification Via Multiobjective Genetic Programming," IEEE Transactions on Neural Networks and Learning Systems, vol.

25, no. 7, pp. 1359-1371, July 2014. doi: 10.1109/TNNLS.2013.2293418.

[5] Y. Luo, T. Liu, D. Tao, C, Xu, "Decomposition-Based Transfer Distance Metric Learning for Image Classification," IEEE Transactions on Image Processing, vol. 23, no. 9, Sept. 2014. doi: 10.1109/TIP.2014.2332398

[6] D. Tao, X. Li, X. Wu, "Maybank S J. Geometric Mean for Subspace Selection," IEEE Transactions on Pattern Analysis and Machine Intelligence, vol. 31, no. 2, pp. 260-274, Feb 2009. doi: 10.1109/TPAMI.2008.70

[7] G. A. Woodell, D. J. Jobson, Z-U Rahman, G. Hines, "Advanced image processing of aerial imagery. Proc SPIE," vol. 6246, pp. 62460E, May 2006. doi:10.1117/12.666767.

[8] J. Han, X. Ji, X. Hu, et al. "Representing and retrieving video shots in human-centric brain imaging space," IEEE Transactions on Image Processing, vol. 22. no. 7, pp. 2723-2736, July 2013. doi:10.1109/TIP.2013.2256919.

[9] J. Han, K. Ngan, M. Li, H. J. Zhang, "A memory learning framework for effective image retrieval," IEEE Transactions on Image Processing, vol. 14, no. 4, pp. 511–524, April. 2005. doi: 10.1109/TIP.2004.841205

[10] D. Tao, X. Tang, X. Li, X. Wu, "Asymmetric Bagging and Random Subspace for Support Vector Machines-Based Relevance Feedback in Image Retrieval," IEEE Transactions on Pattern Analysis and Machine Intelligence, vol. 28, no. 7, pp. 1088-1099, July 2006. doi:10.1109/TPAMI.2006.134.

[11] J. Han, D. Zhang, G. Cheng, L. Guo, J. Ren, "Object detection in optical remote sensing images based on weakly supervised learning and high-level feature learning," IEEE Transactions on Geoscience and Remote Sensing, vol. 53, no. 6, pp. 3325-3337, June 2015. doi:10.1109/TGRS.2014.2374218.

[12] J. Han, P. Zhou, D. Zhang, et al. "Efficient simultaneous detection of multi-class geospatial targets based on visual saliency modeling and discriminative learning of sparse coding," ISPRS J Photogramm Remote Sensing,. vol. 89, pp. 37-48, March 2014. doi:10.1016/j.isprsjprs.2013.12.011.

[13] L. Liu, L. Shao, "Learning Discriminative Representations from RGB-D Video Data," In Proceedings of the Twenty-Third international joint conference on Artificial Intelligence, Beijing, China, 2013, pp. 1493–1500

[14] D. Tao, X. Li X, X. Wu, S. J. Maybank, "General Tensor Discriminant Analysis and Gabor Features for Gait Recognition," IEEE Transactions on Pattern Analysis and Machine Intelligence, vol. 29, no. 10, pp. 1700-1715. doi: 10.1109/TPAMI.2007.1096

[15] Z. Zhang, D. Tao, "Slow Feature Analysis for Human Action Recognition," IEEE Transactions on Pattern Analysis and Machine Intelligence, vol. 34, no. 3, pp. 436-450, March 2012. doi:10.1109/TPAMI.2011.157.

[16] Y. K. Wang, C. T. Fan, "Single Image Defogging by Multiscale Depth Fusion," IEEE Transactions on image processing, vol. 23, no. 11, pp. 4826 - 4837, November 2014. doi: 10.1109/TIP.2014.2358076

[17] T. K. Kim, J. K. Paik, B. S. Kang, "Contrast enhancement system using spatially adaptive histogram equalization with temporal filtering," IEEE Transactions on Consumer Electronics, vol. 4, no. 1, pp. 82-87, Feburary 1998. doi: 10.1109/30.663733

[18] J. Y. Kim, L. S. Kim, S. H. Hwang, "An advanced contrast enhancement using partially overlapped sub-block histogram equalization," IEEE Transactions on Circuits and Systems for Video Technology, vol. 11, no. 4, pp. 475-484, April 2001. doi: 10.1109/76.915354

[19] Y. Y. Schechner, S. G. Narasimhan, S. K. Nayar, "Instant dehazing of images using polarization," in Proceedings of the IEEE Computer Society Conference Computer Vision and Pattern Recognition(CVPR), 2001, pp. 325-332. doi: 10.1109/CVPR.2001.990493

[20] Y. Y. Schechne, S. G. Narasimhan, S. K. Nayar, "Polarization-based vision through haze. Applied Optics," vol. 42, no. 3, pp. 511-525, 2003. doi: 10.1364/AO.42.000511

[21] S. G. Narasimhan, S. K. Nayar, "Contrast restoration of weather degraded images," IEEE Transactions on Pattern Analysis and Machine Intelligence, vol. 25, no. 6, pp. 713–724, June 2003. doi: 10.1109/TPAMI.2003.1201821

[22] S. G. Narasimhan, S. K. Nayar, "Interactive (de) weathering of an image using physical models," in Proceedings IEEE Workshop color Photometric Methods Computer Vision, vol. 6, pp. 1, 2003.

[23] R.T. Tan, "Visibility in Bad Weather from a Single Image," IEEE Conference on Computer Vision and Pattern Recognition, 2008, pp. 1-8. doi: 10.1109/CVPR.2008.4587643

[24] Fattal R, "Single Image Dehazing," ACM Transaction Graph, vol. 27, no. 3, pp. 72, August 2008. doi: 10.1145/1399504.1360671

[25] P. S. JR. Chavez, "An improved dark-object subtraction technique for atmospheric scattering correction of multispectral data," Remote Sensing of Environment, vol. 24, no. 3, pp. 459-479, April 1998. doi: 10.1016/0034-4257(88)90019-3

[26] K. He, J. Sun, X. Tang, "Single Image Haze Removal Using Dark Channel Prior," IEEE Transactions on Pattern Analysis and Machine Intelligence, vol. 33, no. 12, pp. 2341 - 2353, December 2011, doi: 10.1109/TPAMI.2010.168

[27] J. P. Tarel, N. Hautiere, "Fast Visibility Restoration from a Single Color or Gray Level Image," IEEE International Conference on Computer Vision, 2009, pp. 2201-2208 doi: 10.1109/ICCV.2009.5459251

[28] J. M. Liu, Y. G. Hao, Y. B. Zhu, "An Single Image Dehazing Algorithm Using Sky Detection and Segmentation," 7th International Congress on Image and Signal Processing, 2014, pp. 248-252. doi :10.1109/CISP.2014.7003786

[29] K. B. Gibson, D. T. Vo, T. Q. Nguyen, "An investigation of dehazing effect on image and video coding," IEEE Transactions on Image Processing, vol. 12, no. 2, pp. 662-673, Feburary 2012. doi: 10.1109/TIP.2011.2166968

[30] J. Yu, C. Xiao, D. Li, "Physics-based fast single image fog removal," in Proc. IEEE 10th International Conference Signal Process. (ICSP), Oct. 2010, pp. 1048–1052. doi: 10.1109/ICOSP.2010.5655901

[31] K. He, J. Sun, X. Tang, "Guided image filtering," IEEE Transactions on Pattern Analysis and Machine Intelligence , vol. 35, no. 6, pp. 1397-1409, June 2013. doi: 10.1109/TPAMI.2012.213

[32] A. Levin, D. Lischinski, Y. Weiss, "A closed-form solution to natural image matting," IEEE Transaction on Pattern Analysis and Machine Intelligence., vol. 30, no. 2, pp. 228–242, Feburary 2008. doi: 10.1109/TPAMI.2007.1177

[33] W. Bo, Z. Zhihui, Z. Zhiqiang, S. Kang, "Fast Single Image Dehazing Using Iterative Bilateral Filter," 2nd international conference in information engineering and computer science (ICIECS), 2010. doi: 10.1109/ICIECS.2010.5678374

[34] K. Nishino, L. Kratz, S. Lombardi, "Bayesian Defogging," International Journal of Computer Vision, vol. 98, no. 3, pp. 263–278, July 2012. doi: 10.1007/s11263-011-0508-1

[35] F. Guo, H. Peng, J. Tang, "Genetic algorithm-based parameter selection approach to single image defogging," Information Processing Letters, vol. 116, no. 10, pp. 595-602, October 2016. doi: 10.1016/j.ipl.2016.04.013

[36] B. Li, S. Wang, J. Zheng, L. Zheng, "Single image haze removal using content-adaptive dark channel and post enhancement," IET Computer Vision, vol. 8, no. 2, pp. 131-140, April 2014. doi: 10.1049/iet-cvi.2013.0011

[37] A. Shrivastava, Dr. S. Jain, "Single Image Dehazing Based on One Dimensional Linear Filtering and Adaptive Histogram Equalization Method," International Conference on Electrical,

Electronics, and Optimization Techniques (ICEEOT), 2016, pp. 4074-4078. doi: 10.1109/ICEEOT.2016.7755480

[38] Z. Xu, X. Liu, N. Ji, "Fog removal from color images using contrast limited adaptive histogram equalization," 2nd International Conference on Image and Signal Processing, 2009, doi: 10.1109/CISP.2009.5301485

[39] A. Kaur, M. D. Singh, "An Overview of PSO- Based Approaches in Image Segmentation," International Journal of Engineering and Technology, vol. 2, no. 8, pp. 1349-1357, August 2012.

[40] W. N. Chen, J. Zhang, Y. Lin, N. Chen, Z. H. Zhan, H. S. H. Chung, Y. Li, Y. H. Shi, "Particle Swarm Optimization with an Aging Leader and Challengers," IEEE Transactions On Evolutionary Computation, vol. 17, no. 2, pp. 241-258, April 2013. doi: 10.1109/TEVC.2011.2173577

[41] P. P. V. G. D. Reddy, V. Vasavi, M. J. Stephen, "Fingerprint Image Enhancement through Particle Swarm Optimization," International Journal of Computer Applications, vol. 66, no. 21, pp. 1-7, March 2013.

[42] H. K. Ranota, P. Kaur, "A New Single Image Dehazing Approach Using Modified Dark Channel Prior," Advances in Intelligent Systems and Computing, vol. 320, 2015, pp. 77-85. DOI: 10.1007/978-3-319-11218-3_8

